

# Exploiting Scale Invariant Dynamics for Efficient Information Propagation in Large Teams

Robin Grinton, Paul Scerri, Katia Sycara  
Robotics Institute  
Carnegie Mellon University  
rglinton,pscerry,katia@cs.cmu.edu

## ABSTRACT

Large heterogeneous teams will often be in situations where sensor data that is uncertain and conflicting is shared across a peer-to-peer network. Not every team member will have direct access to sensors and team members will be influenced mostly by teammates with whom they communicate directly. In this paper, we investigate the dynamics and emergent behaviors of a large team sharing beliefs to reach conclusions about the world. We find empirically that the dynamics of information propagation in such belief sharing systems are characterized by *information avalanches* of belief changes caused by a single additional sensor reading. The distribution of the size of these avalanches dictates the speed and accuracy with which the team reaches conclusions. A key property of the system is that it exhibits qualitatively different dynamics and system performance over small changes in system parameter ranges. In one particular range, the system exhibits behavior known as *scale-invariant dynamics* which we empirically find to correspond to dramatically more accurate conclusions being reached by team members. Due to the fact that the ranges are very sensitive to configuration details, the parameter ranges over which specific system dynamics occur are extremely difficult to predict precisely. In this paper we (a) develop techniques to mathematically characterize the dynamics of the team belief propagation (b) obtain through simulations the relation between the dynamics and overall system performance, and (c) develop a novel distributed algorithms that the agents in the team use locally to steer the whole team to areas of optimized performance.

## Categories and Subject Descriptors

1.2.11 [Distributed Artificial Intelligence]: Multi-agent systems

## General Terms

Algorithms, Experimentation, Theory

## Keywords

Self-organization, Complex systems, Emergent behavior

## 1. INTRODUCTION

<sup>1</sup> Large heterogeneous teams will often be in situations where sensor data that is uncertain and conflicting is shared across a peer-to-peer network. Not every team member will have direct access to

<sup>1</sup>This research has been sponsored in part by AFOSR FA95500810356.

**Cite as:** Exploiting Scale Invariant Dynamics for Efficient Information Propagation in Large Teams, Robin Grinton, Paul Scerri, Katia Sycara, *Proc. of 9th Int. Conf. on Autonomous Agents and Multiagent Systems (AAMAS 2010)*, van der Hoek, Kaminka, Lespérance, Luck and Sen (eds.), May, 10–14, 2010, Toronto, Canada, pp. 21-28  
Copyright © 2010, International Foundation for Autonomous Agents and Multiagent Systems (www.ifaamas.org). All rights reserved.

sensors and team members will be influenced mostly by teammates with whom they communicate directly. The effective sharing and use of uncertain information is key to the success of large heterogeneous teams in complex environments because without a correct understanding of the environment it is not possible to appropriately plan and act. Typically, noisy information is collected by some portion of the team and shared via the social and/or physical networks connecting members of the team [1]. Each team member will use incoming, uncertain information and the beliefs of those around them to develop their own beliefs about relevant facts. However, the volume of incoming data relative to bandwidth constraints, will often make it impossible for agents to communicate all the received information. Each agent must filter and abstract the information, communicating only its conclusions. Example applications of such systems include large scale disaster relief, environmental monitoring, military crisis response etc. [2].

Before such teams are deployed in domains where there are significant costs for bad behavior, it is important to understand and, if necessary, mitigate any system-wide phenomena that occur during belief propagation. Understanding the dynamics of the system and linking this understanding to overall system performance is difficult since network-based belief propagation in large heterogeneous teams exhibits complex emergent behaviors [3]. Previous attempts to describe the information dynamics of complex systems includes describing propagation of fads [4, 3], rumors [5] and gossip[6] through social networks. The key difference between this work and previous work is that in previous work a single type of information spread whereas here we can have conflicting data that fundamentally changes the dynamics. Moreover, we are able to use agents to predict and control system dynamics in order to guide the team to areas of optimized performance.

To analyze the dynamics, we model a team as being connected via a network with some team members having direct access to sensors and others relying solely on neighbors in the network to inform their beliefs. Each agent uses inference over communications from direct neighbors and sensor data to maintain belief about the environment. The level of abstraction of the model allows for investigation of team level phenomena decoupled from the noise of high fidelity models or the real-world, allowing for repeatability and systematic varying of parameters. Simulation results show that the number of agents coming to the correct conclusion about facts and the speed of their convergence to their belief, varies dramatically depending on factors including network structure and density and conditional probabilities on information communicated from neighbors. As found with similar previous models in the literature, we found that large *avalanches* (or *cascades*) of changes of belief can occur from a single new sensor reading after many previous sensor readings led to no significant change in beliefs of

team members. The model also predicts that the wrong belief can easily cascade through the system, even if an agent knowing all the sensor data to date would have reached the correct conclusion. Such avalanches are due to *double counting*, where agents combine observations of multiple neighbors, incorrectly assuming independence between these observations. This is of great concern in the development of real systems.

We found empirically that when there was an exponential frequency distribution of avalanche sizes, a situation known as *scale invariant dynamics*, there were dramatically fewer instances of propagation of incorrect beliefs. In fact, teams exhibiting belief propagation with scale invariant dynamics can be as much as 50 times more reliable at reaching correct conclusions than teams whose dynamics did not exhibit scale invariance. Moreover, we observed that in the range where the system exhibits scale invariant dynamics, system convergence is much faster than in the other system ranges. While the dramatically increased decision reliability (correctness of the conclusions) makes it highly desirable to have teams exhibit scale invariant belief propagation dynamics, the model predicts that this will occur over relatively small ranges of the relevant system parameters. Minor changes in network structure, conditional probabilities assigned to communications from neighbors and sensor reliability all delicately impact whether scale invariant dynamics occur making it extremely difficult to predict parameter ranges over which scale-invariant dynamics occur.

We performed a mathematical analysis of the model, utilizing techniques from branching processes [7], and determined that the qualitative dynamics of the system are dependent on the value of the *branching factor*. The branching factor is the number of an agent's network neighbors that will change their belief when the agent changes its belief and communicates the change. Scale-invariant dynamics, i.e. areas of high system performance, correspond to an average branching factor of 1. While the individual branching factors of agents vary widely creating the exponential distribution of avalanche sizes, the average of 1 over the team leads to a balance between under- and over-estimating confidence in the propagated information.

In a distributed system where environmental changes and internal system dynamics are complex, local online adaptation to improve overall system performance is highly desirable. Fortunately, since the branching factor can be approximated locally, it can be used to create a local controller that can change system parameters in a way that results in scale invariant dynamics and, hence, in best information propagation. In this paper, we present a local controller that either increases or decreases the conditional probability an agent ascribes to communications from its neighbors depending on its current estimate of its local branching factor. The local controller is shown to make systems starting in a wide range of configurations and with very different emergent dynamics begin to show scale invariant dynamics and improved information propagation performance. We believe that such an algorithm could be used in a practical, large networked heterogeneous agent system (including robots and humans) to dramatically improve the time and reliability with which team members reach correct conclusions based on large volumes of distributed, noisy sensor data.

## 2. MODEL

In this section, we formally describe the underlying model used in the remainder of the paper. The model is intended to be the simplest model that can capture the complex dynamics of uncertain information being shared by a cooperative team. A cooperative team of agents,  $A = \{a_1, \dots, a_{|A|}\}$  are connected by a network,  $G = (A, E)$  where  $E$  is the set of links in  $G$  which connect the

agents in  $A$ . An agent  $a_i$  may only communicate directly with another agent  $a_j \in N_{a_i}$  if  $\exists e_{i,j} \in E$  where we refer to the set  $N_{a_i}$  as its *neighbors*. The average number of neighbors that the agents in  $G$  have is defined as  $\langle d \rangle$  where  $\langle d \rangle = \frac{\sum_i |N_{a_i}|}{|A|}$ .

Sensors,  $S = \{s_1, \dots, s_{|S|}\}$  provide noisy observations to the team. Only one agent can directly see the output of each sensor. The sensors return binary observations about some fact  $b$  from the set  $\{true, false\}$ . In this paper the correct value of the fact is always *true*. We refer to the probability that a sensor  $s$  will return a correct observation as its reliability  $r_s$ . The reliability of a sensor is known to the agent that receives observations from it. In the remainder of this paper, unless otherwise specified,  $|A| = 1000$ ,  $|S| = |A|/20$  and  $r_s = 0.55\forall s$ . That is, most agents must deal with relatively noisy data and do not have direct access to the sensors. For example in military intelligence where only a few intelligence analysts might have direct access to data from sensors like unmanned aerial vehicles.

A key assumption of the model is that it is infeasible for agents to communicate actual sensor observations to one another and that they may only communicate whether they currently believe the fact to be *true, false* or if they are undecided, *unknown*. Although restricting agents to communicating only their conclusions is purely an abstraction to make working with and understanding the model easier, we believe that there are many real world domains where it is infeasible to communicate actual sensor readings. For example, sensor data might be video or audio recordings that are expensive to share on a large network and require significant effort and skill to interpret, or sensor data might be secret, or physical specimens that cannot be shared. If there are large numbers of sensor readings, restricted communication channels and many facts that a large number of agents need to come to conclusions about, we expect it to be infeasible to send most types of raw sensor data.

Each agent  $a_i$  uses either an observation received from a sensor or conclusions about  $b$  communicated by neighbors to form a belief  $P_{a_i}(b \rightarrow true)$  about  $b$ . A new observation is incorporated into the current belief to form a new belief  $P'_{a_i}(b \rightarrow true)$  using Equation 1 an expression of Bayes' Rule.

$$P'(b \rightarrow true) = \frac{P(b \rightarrow true) * cp}{P(b \rightarrow false) * (1 - cp) + P(b \rightarrow true) * cp} \quad (1)$$

Where  $cp = P(b \rightarrow true/o \rightarrow true)$  and  $o$  is an observation. Each observation from a sensor is treated as an independent observation. Only the last communication from any neighbor is treated as an observation. Observations from different neighbors are treated as independent in the application of Bayes' Rule. The treatment of observations of neighbors as independent is not correct, since they may have come to their conclusions based on the same data. Hence, agents relying on neighbors to reach a conclusion will inevitably be over-confident in their conclusions. We refer to this effect as *double counting*. Without communicating actual sensor data or having detailed knowledge of the entire network structure and message sequence, it is impossible to completely remove double counting.

An agent  $a_i$  will communicate *true* if  $P_{a_i}(b \rightarrow true) > \sigma$  and *false* if  $P_{a_i}(b \rightarrow true) < 1 - \sigma$ . Unless otherwise specified  $\sigma = 0.8$ . If the communication causes a neighbor's belief to cross a threshold, it too will communicate with all its neighbors. We refer to this as an *avalanche*. In the simulation of the agent team, when an agent receives a sensor reading, we allow the resulting avalanche to stop propagating before introducing any subsequent sensor readings to the system. The probability  $P(c)$  that  $c$  agents change their

belief during an avalanche is a key measure of the dynamics of the system used throughout the remainder of this paper.

The most important metric for each agent and for the team overall is reliability,  $r_a$  for a single agent and  $R$  for the whole team defined as  $r_a = \text{total correct conclusions} / \text{total incorrect conclusions}$  and  $R = \sum_i r_i / |A|$ . If agents connected to sensors did not communicate until a very large number of sensor readings arrived, they could be very confident their conclusions was correct and the team would be very reliable. However, the team would also be very slow to make decisions and would not leverage the presence of multiple sensors. We use a second metric, convergence time,  $C_n$ , as the time it takes for  $n$  agents to reach the same conclusion. Below, we use  $n = 0.8|A|$ .

### 3. ANALYSIS OF MODEL DYNAMICS

In this section we develop equations that express the dynamics of information propagation in large teams. Specifically we develop equations which relate the system parameters to  $P(c)$ , the probability that an avalanche will encompass  $c$  agents as a result of a single sensor observation.

For this analysis it is assumed that the network  $G$  has a random topology with  $|A| \rightarrow \infty$ . These two assumptions taken in conjunction imply that there are no loops of neighboring agents in the network. These assumptions allow us to formulate avalanches of belief changes in the system as a branching process parameterized by a branching ratio  $\alpha$  [7]. In our system  $\alpha$  is the average number of neighbors of an agent  $a_i$  that change their belief as a result of a belief change communication from agent  $a_i$ . For a given  $\alpha$ ,  $P(c)$  follows directly from the theory of branching processes:

$$P(c) \propto c^{-3/2} \exp\left(-\frac{\omega c}{(1-\alpha)^{-2}}\right) \quad (2)$$

where  $\omega$  is a proportionality constant. In Equation 2,  $c$  is the independent variable, leaving only  $\alpha$ , which is dependent on the system parameters  $cp$  and  $\langle d \rangle$ , to determine overall dynamics.  $\alpha$ , the number of an agent's neighbors changing belief when the agent communicates a new belief averaged over the team, is equivalent to the expected value of the number of neighbors that change belief when a random agent changes belief. This is expressed by Equation 3 where  $p_q$  is the probability that if a random agent changes its belief and communicates with its neighbors,  $q$  of them will change their belief as a result.

$$\alpha = \sum_{q=0}^{\langle d \rangle} qp_q \quad (3)$$

Thus, we know that the probability of an avalanche of a certain size depends on the probability that the belief of a random neighbor exceeds one of the thresholds as a result of receiving a communication. We can compute this value by considering the distribution of possible belief ranges that a neighbor could be in. We discretize the belief  $P(b \rightarrow \text{true}) \in [0, 1]$  of an agent as follows: Let  $F$  represent the belief range  $[0, 1 - \sigma]$  and  $T$  represent the belief range  $[\sigma, 1]$  (an agent with a belief in the former range would communicate *false* and would communicate *true* in the latter range). We define  $n_o$  such that an agent with a belief in either of these ranges would need to receive  $n_o$  observations to enter the opposite belief range. For a fixed value of  $\sigma$ , as  $cp$  increases the number of observations conflicting with its belief that an agent would need for this to occur decreases. Following this intuition  $n_o$  is a function of  $cp$ ,  $n_o(cp)$  which is strictly decreasing with a range  $(1, \infty)$ . Next, we discretize the belief range between the  $F$  and  $T$  ranges into

$n_o$  distinct ranges and associate with these ranges the symbols  $U_0, U_1, \dots, U_{n_o}$ . We can then express the evolution of the beliefs of agents as transitions between these belief ranges due to received communications. Note that, given the preceding definitions,  $U_{n_1}$  and  $U_{n_o}$  are the belief range where a single additional *false* or *true* observation respectively will cause an agent to change belief and communicate the corresponding belief. Define  $P(U_{n_o})$  to be the probability that a random agent will have a belief in the  $U_{n_o}$  range and  $P(U_{n_1})$  the probability that a random agent has a belief in the  $U_{n_1}$  range. Without loss of generality we can define  $P(U_{\text{crit}})$  such that  $P(U_{\text{crit}}) = P(U_{n_o})$  for a *true* sensor observation initiating an avalanche and  $P(U_{\text{crit}}) = P(U_{n_1})$  for a *false* observation. We can then define  $p_q$  in terms of  $P(U_{\text{crit}})$ . Assuming independence between neighbors, the probability that exactly  $q$  neighbors will exceed either threshold is simply the product of the  $q$  individual probabilities,  $P(U_{\text{crit}})$  that a random agent in the team will exceed a threshold after receiving a communication and the  $\langle d \rangle - q$  probabilities  $1 - P(U_{\text{crit}})$  that the remaining neighbors will not exceed the threshold. This relationship is expressed by Equation 4 [8], where the binomial coefficient reflects that neighbors are interchangeable.

$$p_q = \binom{\langle d \rangle}{q} P^q(U_{\text{crit}}) (1 - P(U_{\text{crit}}))^{\langle d \rangle - q} \quad (4)$$

Combining Equations 3 and 4 yields Equation 5:

$$\alpha = \langle d \rangle P(U_{\text{crit}}) \quad (5)$$

which gives the relationship between  $\langle d \rangle$  and  $\alpha$ . To complete the relationship between  $\alpha$  and the remaining system parameters, we need to find the relationship between  $P(U_{\text{crit}})$  and the parameter  $cp$ . We can calculate  $P(U_{\text{crit}})$  by using the mean field assumption that at time  $t$ ,  $P(U_{\text{crit}}) = U_{n_o}(t)$  for a *true* sensor observation and  $P(U_{\text{crit}}) = U_{n_1}(t)$  for a *false* one, where  $U_{n_o}(t)$  and  $U_{n_1}(t)$  are the percentages of agents with belief in the corresponding ranges at time  $t$ . Functions for both  $U_{n_o}(t)$  and  $U_{n_1}(t)$  can be obtained by solving the system of difference equations which express the dynamics of transitions between the belief ranges of the agents as they communicate. These equations are given by:

$$\begin{aligned} F(t+1) &= F(t) - n^t \langle d \rangle F(t) \\ U_i(t+1) &= U_i(t) + n^t \langle d \rangle U_{(i-1)}(t) - n^t \langle d \rangle U_i(t) \\ T(t+1) &= T(t) + n^t \langle d \rangle U_{T_{n_o}}(t) \\ F(t) + \sum_j^{n_o} U_j + T(t) &= 1 \end{aligned} \quad (6)$$

Each equation corresponds to the dynamics of transitions into and out of one of the discrete belief ranges. The equations which govern transitions into and out of the  $U$  belief ranges are identical. To avoid duplication of equations, we include a single generic equation in terms of  $U_i$  where the range of  $i$  is given by  $(1, \dots, n_o)$ . In the equations  $n^t$  is the total number of agents whose belief exceeds a threshold and communicates at time  $t$ . The second equation, for  $i = 2$ , governs the number of agents with a belief in the  $U_2$  range at time  $t + 1$ . This is equal to the number of agents with belief in the  $U_2$  range at time  $t$  plus the number of agents whose belief enters the  $U_2$  range from the  $U_1$  range at time  $t$  as a result of receiving a *true* reading. Subtracted from this is the number of agents that enter the  $U_3$  range at time  $t$ . The number of agents that enter from this belief range from the  $U_1$  range is proportional to  $n^t \propto T(t)$ ,

which is the number of agents that an agent changing its belief communicates with, and the number of agents in the  $U_1$  range. The attractors of the system dynamics correspond to the fixed points of these equations expressed in terms of the percentage of agents having a belief in each range: There is one non-trivial fixed point:  $F(t) = 1/(2n_o + 2)$ ,  $U_i = 1/(2n_o + 2)$  for  $i = 0, 1, \dots, n_o$  and  $T(t) = 0$ . which yields  $P(U_{n_o}) = U_{n_o} = U_{n_1} = 1/n_o(cp) + 2$ . Note that, depending on the type of sensor observation that started the avalanche (*true* or *false*) the signs on the terms in Equations 6 would be opposite. However, such a change from a *true* to a *false* sensor observation simply exchanges the values of  $F(t)$  and  $T(t)$  in the fixed point. The values of either fixed point substituted into Equation 5 yields the same result:

$$\alpha = \langle d \rangle / (n_o(cp) + 2) \quad (7)$$

Recall that  $n_o(cp)$  is the number of sequential observations, having the same truth value, that would be required to change the conclusion of an agent starting with a belief in opposition to those observations. Knowledge of  $\alpha$  allows us to pick values of  $cp$  which give us desired values of  $\alpha$  corresponding to dynamics beneficial to team performance. To this end we calculate  $n_o(cp)$  by empirically inputting values of  $cp$  into Equation 1 and finding the number of observations required to move a prior belief at either end of the belief range to the other end of the range. The result is then integrated over a range of prior beliefs. The resulting plot of  $n_o(cp)$  vs  $cp$  is given by Figure 1. In the next three sections we show that the

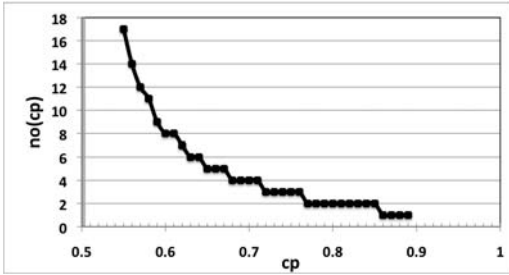


Figure 1: Plot of the function  $n_o(cp)$ .

system exhibits three distinct qualitative dynamics, each resulting in drastically different team performance, depending on the value of  $\alpha$ . Equipped with Equation 7 and Figure 1 we can choose values of  $cp$  and  $\langle d \rangle$  that result in an  $\alpha$  that corresponds with dynamics that give optimal team performance.

### 3.1 Scale Invariant Dynamics

In this section we discuss the qualitative dynamics of the system when parameters  $cp$  and  $d$  are chosen such that  $\alpha = \langle d \rangle / (n_o(cp) + 2) = 1$ . When this condition is satisfied Equation 2 reduces to:

$$P(c) \propto c^{-3/2} \quad (8)$$

This is the defining characteristic of a scale-invariant distribution. Recall that  $n_o(cp)$  is a decreasing function of  $cp$  that gives the number of sequential observations in conflict with its belief that an agent must receive before changing belief. Since the function  $n_o$  is strictly positive and decreasing, for a given value of  $\langle d \rangle$  there is a unique value of  $cp$  that results in  $\alpha = 1$ . When  $P(c)$  is distributed according to Equation 8, a plot of  $\log(P(c))$  vs  $\log(c)$  is a straight line with a slope of  $-3/2$ . A probability distribution with this characteristic is traditionally known as a *scale invariant distribution*. This is because the ratio  $\frac{P(\beta c)}{P(c)}$  for an arbitrary scaling constant  $\beta$  is independent of  $c$ . The practical consequence of this

is that there is no threshold in the size of an avalanche where the probability of an avalanche of that size becomes zero. This means when the dynamics of the system are governed by Equation 8 there is a significant probability that avalanches of all sizes will occur. However, Equation 8 also tells us that small avalanches will occur relatively much more frequently than large ones. We refer to the dynamics expressed by Equation 8 as *scale invariant dynamics*.

We conducted an experiment to test the validity of Equation 8 as a qualitative description of the dynamics of the system when  $\alpha = 1$ . We simulated the system using parameter value  $|S| = 1/20|A|$ ,  $\langle d \rangle = 8$ , and  $|A| = 1, 000; 10, 000; 50, 000$ . With  $\langle d \rangle = 8$ , we found from the plot of Figure 1 and Equation 7 that  $cp = 0.63$  gives  $\alpha = 1$ , and used this value in the experiment. The results for other values of  $\langle d \rangle$  and the corresponding  $cp$  that give  $\alpha = 1$  were similar but we omitted them to conserve space. Figure 2 shows the resulting plot of the log of the frequency that an avalanche of a certain size occurred during 10000 simulations of the system vs. the log of the size of the avalanche. Included

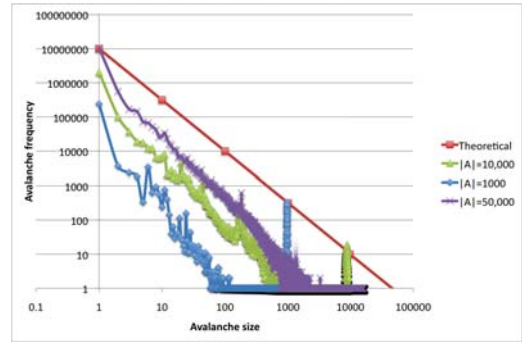


Figure 2: The avalanche distribution approaches the theoretical distribution as  $|A|$  is increased.

in the figure is the theoretical prediction of a straight line with a slope of  $-3/2$  given by Equation 8. We see from the figure that as the number of agents  $|A|$  is increased, the avalanche distributions approach the theoretical distribution. This is to be expected as the analysis was conducted with the assumption of a system of infinite size.

### 3.2 Stable Dynamics

In this section we discuss the qualitative dynamics of the system when  $\alpha = \langle d \rangle / (n_o(cp) + 2) < 1$ . For parameter ranges that satisfy this inequality Equation 2 reduces to Equation 9:

$$P(c) \propto c^{-3/2} \exp\left(-\frac{c}{(1 - \langle d \rangle / (n_o(cp) + 2))^{-2}}\right) \quad (9)$$

In this parameter range the exponential factor shown in Equation 9 has a negative sign, which means that the probability of larger avalanches relative to the system size drops dramatically. This is in stark contrast to the scale invariant dynamics where avalanches of all sizes were probable. Equation 9 tells us that perturbations to the system caused by sensor inputs are quickly curtailed. For this reason we refer to these dynamics as *stable dynamics*.

We conducted an experiment to test the validity of Equation 9 as a qualitative description of the dynamics of the system when  $\alpha < 1$ . We simulated the system using parameter value  $|S| = 1/20|A|$ ,  $\langle d \rangle = 4$ , and  $|A| = 1, 000$ . With  $\langle d \rangle = 8$ , we found from Equation 7 that  $cp < 0.63$  gives  $\alpha < 1$ . Figure 3 shows the resulting plot of the log of the frequency that an avalanche of a certain size occurred during 10000 simulation runs of the system

vs. the log of the size of the avalanche. The figure shows the result when  $cp = 0.55$  but other values of  $cp < 0.63$  give similar results.

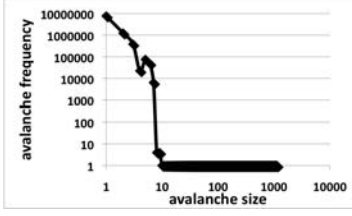


Figure 3: Avalanche Distribution for  $\alpha < 1$ .

### 3.3 Unstable Dynamics

In this section we discuss the qualitative dynamics of the system when  $\alpha = \langle d \rangle / (n_o(cp) + 2) > 1$ . For parameter ranges that satisfy this inequality Equation 2 reduces to Equation 10:

$$P(c) \propto c^{-3/2} \exp\left(\frac{c}{(1 - \langle d \rangle / (n_o(cp) + 2))^{-2}}\right) \quad (10)$$

Equation 10 is identical to 9, except the sign on the exponential term is positive. Consequently, in this parameter range large avalanches are enhanced and are much more probable than in the other parameter ranges.

We conducted an experiment to test the validity of Equation 10 as a qualitative description of the dynamics of the system when  $\alpha > 1$ . We simulated the system using parameter values  $|S| = 1/20|A|$ ,  $\langle d \rangle = 4$ , and  $|A| = 1,000$ . With  $\langle d \rangle = 4$ , we found from Equation 7 that  $cp > 0.63$  gives  $\alpha > 1$ . We used the value  $cp = 0.8$  for this experiment. Figure 3 shows the resulting plot of the log of the frequency that an avalanche of a certain size occurred during 10000 simulation runs of the system vs. the log of the size of the avalanche. We see from Figure 4 that the system

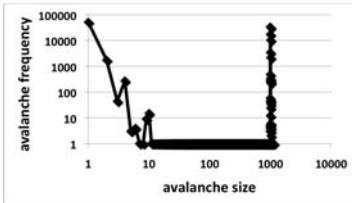


Figure 4: Avalanche Distribution for  $\alpha > 1$ .

behavior is in good agreement with the qualitative prediction of Equation 10. The figure shows that almost 50% of the avalanches that occurred during 10000 simulation runs were of size 1000, the system size.

## 4. PERFORMANCE OF DYNAMICS

We found empirically that the performance of the team measured by the metric  $R$  was up to 1000 times better than in other parameter ranges, when the parameter  $cp$  was chosen relative to  $\langle d \rangle$  such that  $\alpha = 1$  and the avalanche distribution was governed by the scale-invariant distribution given by Equation 8. Furthermore, the convergence time  $C_{800}$ , the time for 0% of the team to come to the correct conclusion, was simultaneously very low. This result, shown in Figure 5, is the result of an experiment where we investigated the average reliability  $R$  and the convergence time  $C_{800}$

as a function of  $cp$  the conditional probability that agents assign to communication from their neighbors. The experiment was conducted using  $|S| = 1/20|A|$  and  $\langle d \rangle = 8$ . The figure shows that the team's performance is clearly optimized for  $cp = 0.63$ . From Figure 1,  $n_o(0.63) = 6$ . Plugging into Equation 7 yields,  $\alpha = 8/(6 + 2) = 1$  which corresponds with scale invariant dynamics. We also see that the performance of the team, measured via both reliability and convergence time, is extremely sensitive to  $cp$ . The figure shows how  $R$  peaks dramatically while  $C_{800}$  is very small. As  $cp$  is increased, reliability goes up at first slowly and then very dramatically before falling off even more dramatically. The convergence time drops dramatically at the high end of the  $cp$  spike. Notice that for high  $cp$ ,  $C_{800}$  is high because there is not agreement by 80% of the team even after a long period. The opti-

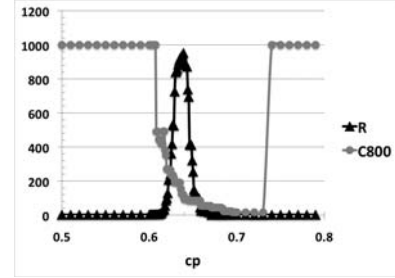
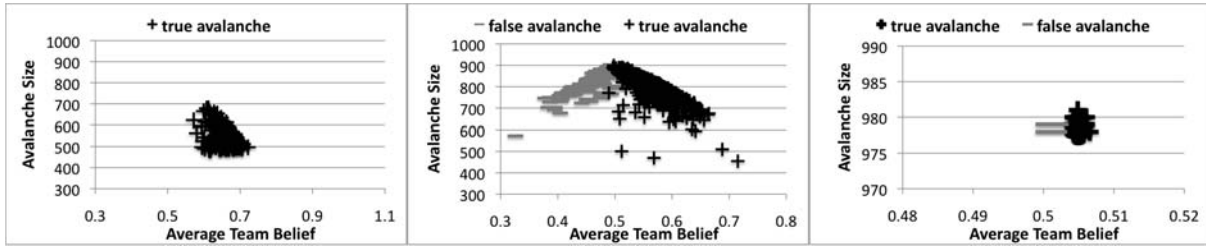


Figure 5:  $R$  vs  $cp$ , the peak which is several orders of magnitude larger than the surrounding points occurs at  $\alpha = 1$ .

mal reliability for  $cp = 0.63$  and  $\alpha = 1$  can be understood in terms of the system dynamics. The frequent smaller avalanches prevent the system from overreacting to incorrect data, however though less frequent, large avalanches occur and disseminate these locally vetted decisions to the rest of the system. These local decisions then mix further improving the conclusions that agents come to. This hypothesis is supported by the results given by Figure 6. This Figure shows a scatter plot of the size of an avalanche against the average belief of the team in the previous time step:  $\frac{\sum_i P_{a_i}(b \rightarrow true)}{|A|}$  (only avalanches that encompassed more than 50% of the team were included, smaller avalanches were omitted to make the figure readable). The points in the plot were also split by the decision *true* or *false* being propagated by the avalanche represented by a point. The leftmost plot of Figure 6 shows that when  $cp = 0.63$ , the large avalanches exclusively propagate the correct belief of *true*. This supports the assertion that the frequent small avalanches allowed agents near to the sensors to come to more reliable conclusions which were then disseminated by avalanches of correct decisions. We see from Figure 3 that the system behavior is in good agreement with the qualitative prediction of Equation 9. The figure shows that avalanches of size greater than 10 never occurred during the 10000 simulation runs of the system.

Figure 5 shows that reliability of agent decisions as measured by  $R$  is extremely poor for stable dynamics (when  $cp < 0.63$  and  $\alpha < 1$ ). These results can be explained by the dynamics of the system in this parameter range as expressed by Equation 9. Performance in this range is poor because only relatively few agents, the ones separated from a sensor in the network by only a small number of intermediate agents, ever receive any information. This also explains the high convergence time. Small avalanches means that there is never a consensus among a significant portion of the team.

Figure 5, shows that the reliability of agents decisions is low in this parameter range ( $cp > 0.63$  and  $\alpha > 1$ ) This poor performance is due to the bias towards large avalanches in this range. This bias means that an avalanche started by a single new sensor



**Figure 6: When  $\alpha = 1$  large avalanches only propagate correct information.**

reading will, with high probability, encompass a large percentage of agents in the system, including agents who have previously come to a decision that contradicts the new sensor reading. With a low sensor reliability ( $s_r = 0.55$  in this paper), sequential sensor readings will often be conflicting and consequently agents will change belief often. These frequent changes means that the decisions of individual agents do not reflect the trend in the data, instead they reflect the sensor reading that triggered the last avalanche which reached that agent. The consequence is that the sensor reliability is an upper bound on the average reliability of the system. This also explains the high convergence time in this region. To converge to a stable decision in this parameter range, an agent will need to receive a stream of consistent observations. The probability of this occurring is very low and consequently will take a long time to occur. Because of the instability of the decisions of agents in this parameter range, we refer to these dynamics as *unstable dynamics*. This assertion is supported by the rightmost two plots of Figure 6. These were generated in the exact same manner as the leftmost plot except  $cp$  is set to 0.7 and 0.8 respectively. These figures show that for  $\alpha > 1$  large avalanches frequently disseminate both correct and incorrect decisions to large portions of the team. We can also see that as  $cp$  increases, these large avalanches increasingly occur when agents are very uncertain (average team belief  $\approx 0.5$ ) meaning that the system is becoming increasingly unstable.

## 5. NETWORK VARIATION

The analysis of Section 3 made a key assumption about the network to simplify the mathematics of specifying the relationship between  $\alpha$ , which characterizes system dynamics and system parameters  $cp$  and  $\langle d \rangle$ . This assumption was of an infinite random network with no loops of neighboring agents. Furthermore, the analysis implicitly assumed that  $\langle d \rangle$ , the average number of links per node, is an accurate characterization of the local structure of a network by making use of it in probability calculations of agent interactions. However, other communication network structures that might be used in real-world teams, deviate significantly from these assumptions. In this section, we empirically investigate variations from the predictions of Section 3 that result when other communication network structures are employed.

A particularly surprising result stemming from our investigation was that even networks generated with the same generating function exhibited dramatic differences in average performance of the network. Figure 7 shows the distribution of reliability and convergence times for 100 instances of a scale-free network generated with exactly the same parameters. 10,000 runs are used to generate each point and the same random seed for generating sensor data is used to minimize noise in the results. A  $cp$  of 0.68 was used, having been found to be a good value for this type of network. The networks are statistically very similar, the only differences are minor linking differences caused by randomness in the

generation process. Notice that there is a difference of up to a factor of 20 between the best and worst performing networks. This indicates that minor topological details are important as well as the general structure. This is in contrast with the predictions of Section 3 that  $\alpha$ , the value of which was found to be an important indicator of performance, is uniquely determined by  $\langle d \rangle$  for a fixed value of  $cp$ . This discrepancy is likely due to the fact that  $\langle d \rangle$  does not accurately reflect the local structure of a ScaleFree network. Unlike, a large random network where the variance on  $\langle d \rangle$  would be very low, for a ScaleFree network the variance of  $\langle d \rangle$  is very high. This means that although the networks shown in Figure 7 have similar values of  $\langle d \rangle$ , the minor topological differences cause variances differences which in turn impact the value of  $\alpha$  and performance. The performance of a particular

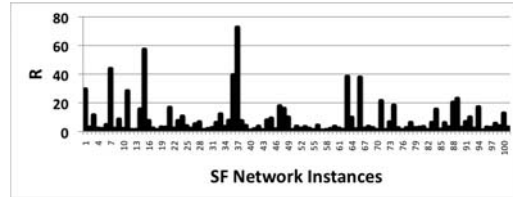


**Figure 7: Variation of  $R$  within 100 instances of ScaleFree networks generated with the same stochastic parameters.**

team also turns out to be very sensitive to the particular characteristics of the network connecting them. To investigate the differences in performance between networks generated with different generating functions we conducted experiments to in which we looked at performance differences between different network types as link density  $\langle d \rangle$  is varied. The networks used in the experiment are generated from standard generation algorithms and were chosen to represent a range of possibilities that may occur in real systems. For each of the network types, we found the  $cp$  value (to the nearest 0.02) that maximized the performance as measured by the metric  $R$  for 100 networks of that type. Then the 100 networks of each type was run 1000 times and the average performance computed. Figure 8 shows the average reliability  $R$  of all the networks. Figure 9 shows the best  $cp$  value for each network type and corresponding density  $\langle d \rangle$ . The network types are abbreviated in the table as R for Random, SF for ScaleFree, SWG for SmallWorldGrid, and SWR for SmallWorldRing respectively. Two things are clear from the figures. First, some general network structures are better than others. The difference in performance between network types is both due to the differences in variance in  $\langle d \rangle$  between different network structures as well as the degree to which agents in a particular network type tend to share neighbors, creating loops of agents. When an agent's neighbors share mutual ancestors that are a part of an avalanche, the same avalanche might reach that agent multiple times. The result is an increase in the probability that the agent will

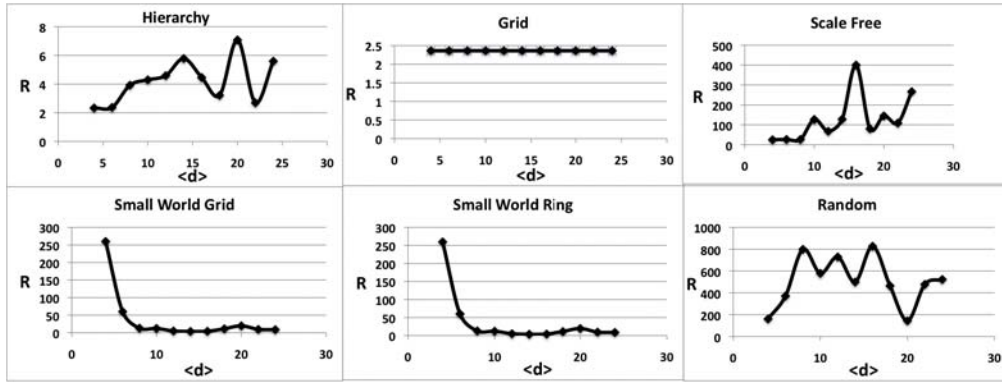


Figure 8: Variation of  $R$ , and  $C_{800}$  with network type and density  $\langle d \rangle$ .

receive enough observations to change belief and continue propagating the avalanche. This effect will tend to offset the scale invariant dynamics by increasing the proportion of large avalanches in the avalanche distribution. The result is a decrease in performance depending on the degree to which the network structure forms loops of agents. This is a possible explanation for the relatively poor performance of the Grid network structure which contains many loops of agents.

Networks with a *small worlds* property performed better than those without. This is possibly because the small worlds property of the network enhances the scale invariant dynamics which we have shown to be beneficial to team performance. These networks have highly structured local subnetworks and these local subnetworks are joined by a few random links. The dense local subnetworks mean that most information exchange occurs locally, while the few random links which join them encourage mixing between regions generated in local subnetworks.

The average degree of the network makes less of a difference to overall performance than the type, but for most network types it dramatically influences the best  $cp$  for that network. In addition, for a particular network type, the best  $cp$  drops as  $\langle d \rangle$  increases. This can be explained qualitatively by the expression for  $\alpha$ :  $\alpha = \langle d \rangle / ((n_o(cp) + 2))$ . Recall that  $n_o(cp)$  is a decreasing function of  $cp$ . From the expression for  $\alpha$  we can see that as  $\langle d \rangle$  increases  $\alpha$  increases moving away from 1. Decreasing  $cp$  increases  $f$  which in turn decreases  $\alpha$  back towards 1 where performance is optimal. The high level conclusion from this experiment is that deviations in the network from the idealization used in the analysis of Section 3 means that it is very difficult to calculate the values of  $cp$  for a given network that results in good performance.

$\langle d \rangle$	4	6	8	10	16	18	24
SF	0.70	0.62	0.60	0.58	0.58	0.58	0.56
R	0.74	0.66	0.63	0.62	0.58	0.58	0.56
SWG	0.72	0.72	0.72	0.72	0.70	0.74	0.72
SWR	0.72	0.72	0.72	0.72	0.70	0.74	0.72

Figure 9: The value of  $cp$  that results in the highest value of decision reliability  $R$  for each network type/link density  $\langle d \rangle$ .

## 6. INTERACTION MANAGEMENT

The analysis of Section 3 shows that the communication dynamics of a network of cooperative agents will follow one of three qualitatively different avalanche distributions namely, *stable*, *scale invariant*, and *unstable*, depending on the values of the parameters  $\langle d \rangle$  and  $cp$ . This section also showed that of these three avalanche

distributions, the scale invariant avalanche distribution expressed by Equation 8 is optimal in terms of the reliability of agent decisions  $R$ . However, the experiments of Section 5 showed that the variance on  $\langle d \rangle$  has a dramatic effect on  $\alpha$  and hence performance, even between networks generated using the same generating functions. For real systems the network structure is given and hence  $\langle d \rangle$  and its variance are also given. However because of the complexity of such systems it would be very difficult in practice to determine  $\langle d \rangle$  with enough precision to pick the corresponding  $cp$  that would result in the highest possible performance. Furthermore, real systems are dynamic, meaning that the values of  $\langle d \rangle$  and its variance are likely to change over time which would in turn also change the  $cp$  that would give optimal performance. The key observation however is that  $\alpha = 1$  results in scale invariant dynamics and optimal performance. To overcome the practical difficulties in picking the best  $cp$  for a network we developed a distributed algorithm called DACOR (Distributed Adaptive Communication for Overall Reliability) that an agent  $a_i$  can use to dynamically tune its  $cp$  to achieve a local branching ratio of  $\alpha_{a_i} = 1$  in an attempt to cooperatively achieve  $\alpha = 1$  resulting in optimal performance for the team. The pseudocode for DACOR is given by Algorithm 6. In line 1 of the algorithm the agent calcu-

### Algorithm 1: tune local branching ratio.

```

DACOR()
(1)  $\alpha_a = (\alpha_a * (uA - 1) / uA) + (pC / uA)$ 
 $\Delta\alpha = \alpha_a - 1$ 
(2) foreach  $a_j \in N$ 
(3)  $a \rightarrow \text{SENDMESSAGE}(a_j, \Delta\alpha)$ 
(4)  $a_j.cp = a_j.cp(\Delta\alpha) * \gamma - (\Delta\alpha') * \beta$ 
(5) if  $a_j.cp > cp_{max}$ 
(6)  $a_j.cp = cp_{max}$ 
(7) else if  $a_j.cp < cp_{min}$ 
(8)  $a_j.cp = cp_{min}$ 

```

lates its local  $\alpha$ , where  $pC$  is the number of the agent's neighbors that changed belief and  $uA$  is a factor that weights more recent local observations of  $\alpha$  higher in the average. In lines 2-3 the agent then sends its approximation of the local  $\alpha$  to its neighbors. In line 4 the agent's neighbors then update their  $cp$  values proportional to  $\Delta\alpha = \alpha - 1$  and its derivative  $\Delta\alpha'$ . The remaining lines are to ensure that the neighbors  $cp$  values remain in the range  $[0,1]$  since  $cp$  is a probability. We ran an experiment to test the efficacy of DACOR in tuning  $cp$  to improve the performance of the agent team. We used  $|A| = 1000$ ,  $|S| = 50$ , and  $\langle d \rangle = 4$ . In the experiment we hand tuned  $cp$  to give the best performance for several different network types. Next we allowed the agents to tune  $cp$  using DACOR. Each result using DACOR is an average over 100 simulation

network type	$R$ tuned	$C_{800}$ tuned	$R$ DACOR	$C_{800}$ DACOR
ScaleFree	1.62	14.00	1.27	13.00
Small World Ring	1.43	244.00	1.08	7.00
Random	16.00	61.00	12.57	61.00

Figure 10: Comparison between performance of teams using hand tuned  $cp$  vs  $cp$  tuned by agents running DACOR.

runs, with a randomly chosen initial  $cp$ . The results are shown in Figure 10.

## 7. RELATED WORK

There have been several studies conducted to investigate models whose dynamics are governed by cascades on complex networks. These include models of fads[4, 3], rumors [5], gossip[6], forest fires [9], and diseases[10, 11]. Common to all of these models is that the dynamics are governed by the spreading of a single influence. In contrast, our model investigates competing influences which significantly alters the dynamics of a system. Many of the systems under study in these studies fall into the category of self-organized critical systems, which exhibit scale invariant dynamics over large parameter ranges[12]. In contrast, we found that very small changes in the conditional probability assigned to information from neighbors in our model could cause the team to exhibit other types of dynamics.

In [13], Parunak presents a model of the collective convergence of agents to a cognitive state. This model is similar to ours in that it does include multiple states that agents can converge to and hence competition between states. In addition, similar to our work, Parunak also uses a mean field approach to simplify analysis of the system. Parunak focuses on studying the macroscopic performance of the system. We build upon Parunak’s investigation by analyzing the dynamics of the system directly and investigating the relationship between the dynamics and the performance of the system. Our work further investigates a distributed algorithm for encouraging dynamics which are beneficial to system performance.

Recently there has been significant interest in social networks [14], [15] and the impact of those networks on performance of a group. For example, Xu looked at the impact of networks on routing information to a specific agent [16]. Kleinberg, looked at the impact of the network on the performance of decentralized search algorithms [17], when a single agent has information valuable to the system. We build on both of these contributions by investigating the case when a large percentage of the agents in the team are both sources and sinks for information, which fundamentally changes the dynamics of information exchange in the system. Boyd has looked at the impact of networks on decentralized gossip-based information dissemination [6], our analysis method could be utilized to understand the dynamics of information exchange in Boyd’s model.

## 8. CONCLUSIONS AND FUTURE WORK

This paper presented a model that suggests that when a network of cooperative agents exhibits scale invariant dynamics, the speed and reliability with which the team can converge to correct conclusions, despite noisy data and highly limited communication is dramatically increased. Unfortunately, theoretical predictions of parameter values over which scale-invariant dynamics occur is predicated on an infinite random network. We showed that deviations of some network types and configurations from this ideal makes it extremely difficult to select parameter values that result in scale-invariant dynamics. We further, showed that performance varied greatly depending on network type and that there was considerable variance even for very similar networks. To overcome the diffi-

culties of parameter selection for scale invariant dynamics, the paper presented an algorithm that allows agents to make local adjustments to conditional probabilities on neighbors observations that move the team towards the parameter range where scale invariant dynamics occur for any network type, thus dramatically improving its performance. This algorithm minimizes disruptions to the overall network, making it practically applicable in real world systems.

In future work, we propose to extend the model to capture additional features of information sharing, including beliefs of several variables and a richer communication model, while maintaining the mathematical simplicity that allows the types of detailed analysis above. We also intend to simulate features that are harder to model mathematically, such as the ways mobile sensors might be redeployed based on initial conclusions and how other coordination activities can influence belief convergence.

## 9. REFERENCES

- [1] B. Bellur, M. Lewis, and F. Templin, “An ad-hoc network for teams of autonomous vehicles,” in *Proceedings of the First Annual Symposium on Autonomous Intelligence Networks and Systems*, 2002.
- [2] J. Casper and R. Murphy, “Human-robot interaction during the robot-assisted urban search and rescue effort at the world trade center,” vol. 33, pp. 367–385, 2003.
- [3] W. DJ, “A simple model of global cascades on random networks,” *Proceedings of the National Academy of Science*, vol. 99, pp. 5766–5771, 2002.
- [4] S. Bikhchandani, D. Hirshleifer, and I. Welch, “A theory of fads, fashion, custom, and cultural change as informational cascades,” *Journal of Political Economy*, vol. 100, no. 5, p. 992, 1992.
- [5] M. Nekovee, Y. Moreno, G. Bianconi, and M. Marsili, “Theory of rumour spreading in complex social networks,” *Physica A: Statistical Mechanics and its Applications*, vol. 374, no. 1, pp. 457–470, 2007.
- [6] S. Boyd, A. Ghosh, B. Prabhakar, and D. Shah, “Randomized gossip algorithms,” *IEEE/ACM Trans. Netw.*, vol. 14, no. SI, pp. 2508–2530, 2006.
- [7] T. Harris, *The theory of branching processes*. Springer, 1963.
- [8] K. Christensen and Z. Olami, “Sandpile models with and without an underlying spatial structure,” *Phys. Rev. E*, vol. 48, no. 5, pp. 3361–3372, Nov 1993.
- [9] S. Clar, B. Drossel, and F. Schwabl, “Scaling laws and simulation results for the self-organized critical forest-fire model,” *Phys Rev E*, vol. 50, p. 1009D1018, 1994.
- [10] R. Pastor-Satorras and A. Vespignani, “Epidemic spreading in scale-free networks,” *Phys. Rev. Lett.*, vol. 86, no. 14, pp. 3200–3203, Apr 2001.
- [11] V. M. Egufluz and K. Klemm, “Epidemic threshold in structured scale-free networks,” *Phys. Rev. Lett.*, vol. 89, no. 10, p. 108701, Aug 2002.
- [12] P. Bak, C. Tang, and K. Wiesenfeld, “Self-organized criticality: an explanation of  $1/f$  noise,” *Physical Review Letters*, pp. 381–384, 1983.
- [13] V. Parunak, “A mathematical analysis of collective cognitive convergence,” in *AAMAS ’09*, 2009, pp. 473–480.
- [14] D. Watts and S. Strogatz, “Collective dynamics of small world networks,” *Nature*, vol. 393, pp. 440–442, 1998.
- [15] A.-L. Barabasi and E. Bonabeau, “Scale free networks,” *Scientific American*, pp. 60–69, May 2003.
- [16] Y. Xu, P. Scerri, B. Yu, S. Okamoto, M. Lewis, and K. Sycara, “An integrated token-based algorithm for scalable coordination,” in *AAMAS’05*, 2005.
- [17] J. Kleinberg, “Complex networks and decentralized search algorithms,” in *(ICM)*, 2006.